CH_4 Activation by W Atom in the Gas Phase: A Case of Two-State Reactivity Process

YongCheng Wang,* Qiang Wang, ZhiYuan Geng, LingLing Lv, YuBing Si, QingYun Wang, HuiWen Liu, and DanDan Cui

College of Chemistry and Chemical Engineering, Northwest Normal University, Lanzhou, Gansu 730070, P. R. China

Received: June 10, 2009; Revised Manuscript Received: September 12, 2009

Gas-phase methane activation by tungsten (W) atoms was studied at the density functional level of theory using the hybrid exchange correlation functional B3LYP. Four reaction profiles corresponding to the septet, quintet, triplet, and singlet multiplicities were investigated in order to ascertain the presence of some spin inversion during the methane activation. Methane activation mediated by W atoms was found to be a spin-forbidden process resulting from the crossing among the multistate energetic profiles. On the basis of the Hammond postulate, this is a typical two-state reactivity (TSR) reaction. The minimum energy crossing points lead to decrease in the barrier heights of TS01, TS12, TS23, and TS24 that correspond to the first, second, and third hydrogen transfer and the reductive elimination step of H_2, respectively. The spin−orbit coupling is calculated between electronic states of different multiplicities at the crossing points (MECPs) to estimate the intersystem crossing probabilities, and the probability of hopping from one surface to the other in the vicinity of the crossing region is calculated by the Landau−Zener type model.

1. Introduction

The effective use of methane as a raw material for industrial applications remains one of the long-standing problems in catalysis. Over the past several years, several different direct and indirect routes for the methane conversion to value-added products, such as higher hydrocarbons and oxygenates, have been considered because of the high economical, environmental, and political impact that this process may cause.[1−3] The selective transformation of common inert C−H bonds of alkanes such as methane to other functional groups by neutral transition metals to give high oxidation state transition metal complexes has been motivated by both interest in the fundamental aspects of the chemistry and the potential economic and environmental impact of this chemistry.[4] Thus, there have been many experiments and theoretical calculations in this area, which has resulted in many examples in the literature of C−H bond activation at transition metal centers.[4−6] The activation of methane by a neutral transition metal has been the subject of a number of studies in order to get better understanding of the practical alkane conversion processes.[7−9] High oxidation state transition metal complexes containing a carbon−metal double bond or triple bond are important for understanding the nature of metal coordination and for developing catalysts in alkene metathesis and alkane activation reactions.[10−12] The activation of methane has always been a challenge to chemists.

Previous studies on the reactions between transition metal atoms and methane have shown that inversion of the C−H bond of methane is more facile for metal cations than for neutral metal atoms.[13,14] In contrast, there have been relatively few reports involving the reaction of neutral transition metal atoms with small alkanes. However, recent reactions of laser-ablated group IV, V, and VI transition metal atoms with methane and methyl halides have generated a new class of small insertion products and high-oxidation-state complexes with multiple carbon−metal bonds.[15−21] To our knowledge, a recent experimental report of W + CH_4 was given by Andrews' group,[21] who formed the trihydrido methylidyne complex $CH{\equiv}WH_3$ in excess argon. These workers also computed B3LYP energies, frequencies, and structures to support their assignment to this lowest energy product, but they did not take into account reaction path and a possible spin inversion process. To explore and gain insight into the mechanism of the reaction, we have investigated the potential energy surfaces (PESs) crossing points associated with the C−H activation of methane by W atoms by means of density functional theory (DFT). Methane dehydrogenation by bare transition metals is one of the most common reactions involving a transition element and an alkane in the gas phase. Great efforts have been spent in the past decade on experimental and theoretical investigations for this type of reaction.[22−29] In the present study, we have made a theoretical prediction about methane dehydrogenation by a neutral tungsten atom in the gas phase. Thermal reactions that include more than one spin PES are becoming the topic of increasing interest.[30,31] The spin-forbidden reactions that involve a change in the spin state and thus occur on two or more PESs are known to be important in determining the outcome of chemical processes.[32,33] We found that C−H activation of methane by W atoms involves "two-state reactivity" based on our DFT calculations. To better understand the spin inversion processes involved in the C−H bond activation reaction, we determined the energies and structures of the crossing points between the two PESs of different spin states in the reaction pathway. The effect of the crossing points on the energy barriers of the different reaction pathway steps is discussed. The calculated energy pathway is in good agreement with the theoretical result from Andrews' group.[21] Also, we believe that the results reported here provide new insights into the title reaction.

2. Computational Details

Computations were carried out with the Gaussian 03 program package.[34] Energies and geometries of the reaction intermediates

* Corresponding author. Fax: +86-0931-7971989. E-mail: ycwang@163.com.

10.1021/jp9054439 CCC: $40.75
Published on Web 10/28/2009

and transition states were calculated using the Becke's three parameter hybrid functional[35,36] combined with the Lee, Yang, and Parr (LYP) correlation functional,[37] denoted as B3LYP. In all of the calculations, the 6-311++G (3df, 3pd) basis set was used for the carbon and hydrogen atoms,[38] and for the relativistic effective core potential (RECP) of Stuttgart on W, the 5d and 6s in W are treated explicitly by a (8s7p6d) Gaussian basis set contracted to (6s5p3d). With respect to Hessians (matrix of energy second derivatives), local minima on a PES have no negative eigenvalue and saddle points have a single negative eigenvalue. The intrinsic reaction coordinate (IRC) was then calculated and used to track the minimum energy path from transition states to the corresponding minima, to probe the reaction path and check if the correct transition state was located.

To locate the crossing points (CPs) between states of different spin multiplicities, the procedure used by Yoshizawa et al.[39] has been selected. Starting from the TS closest to the crossing seams, the IRC path was traced down to the corresponding minimum. Thereafter, each optimized point along the IRC path was submitted to a single point energy calculation with the other electronic state. The set of CPs we obtain in this way can be considered as estimates of the minimum energy crossing points (MECPs) between the multistate hypersurfaces. The mathematical algorithm to obtain MECPs proposed by Harvey et al.[40] has been also employed.

Approximate one-electron spin−orbit coupling (SOC) calculations have been carried out with the GAMESS[41] suite of programs, using the effective one-electron SO operator:[42]

$$\hat{H}_{\mathrm{SO}} = \frac{\alpha^2}{2} \sum_i \sum_k \left(\frac{Z_k^*}{r_{ik}^3} \right) (\hat{S}_i \cdot \hat{L}_{ik}) = \sum_i h_i(Z^*) \qquad (1)$$

$$\frac{\alpha^2}{2} = \frac{e^2 h}{4\pi m_e^2 c^2} \qquad (2)$$

Where $\hat{L}_{ik}$ and $\hat{S}_i$ are the orbital and spin angular momentum operators for the ith electron in the framework of the nuclei, indexed by K. To account for the missing two-electron part of the Hamiltonian, the nuclear charge Z_K is replaced by an effective parameter, Z_K*, which can be taken as the screened nuclear charge.

In the semiclassical picture based on PESs, the probability of intersystem crossing (ISC) for a molecule passing through two different spin states crossing in a Landau−Zener type model is given by[43,44]

$$P^{\mathrm{ISC}} = 1 - P^{\mathrm{LZ}} \qquad (3)$$

$$P^{\mathrm{LZ}} = \exp\left(-\frac{\pi}{4} \xi \right) \qquad (4)$$

$$\xi = \frac{8(\mathrm{SOC})^2}{\hbar \vec{g}d \vec{v} N_{\mathrm{AV}}} \qquad (5)$$

Here, SOC is the matrix element between the two spin situations, $\vec{g}d$ is the gradient difference vector between the two different states and $\vec{v}$ is the velocity of the molecule at the crossing point.

3. Results and Discussion

The potential energy profiles for the septet, quintet, triplet, and singlet states were determined to investigate the possible spin crossovers involved in the reaction pathways. The geometries of the stationary points at the septet, quintet, triplet, and singlet states are depicted in Figure 1, and the calculated potential energy profiles are presented in Figures 2 and 3.

3.1. Overview of the Potential Energy Surfaces. ***3.1.1. Septet Surface of the Reaction.*** As for the septet surface, ^{7}IM0 is initially formed as ^{7}W collides with CH_4. Then the hydridomethyl complex ^{7}IM1 is formed via the first H transfer through the transition state ^{7}TS01, with a reaction barrier of 36.4 kcal/mol. Subsequently, the second and third H transfer reactions take place on the corresponding complexes via transition states ^{7}TS12 and ^{7}TS23, with barriers of 45.2 and 43.6 kcal/mol, respectively. The overall reaction on this pathway is endoergic by 67.1 kcal/mol, which is not easy to take place for the reaction because of the presence of the high activation barriers. ^{7}IM2 is complex $(H_2)WCH_2$. The bond distance between the two hydrogen atoms in the H_2 unit is 0.804 Å, which is slightly longer than the H−H bond of H_2 in the gas phase, that is, 0.743 Å. Therefore, ^{7}IM2 can probably eliminate a hydrogen molecule, and the overall H_2 elimination reaction starting with the CH_4 + W (^{7}S) reactants is endothermic, by 43.9 kcal/mol.

3.1.2. Quintet Surface of the Reaction. Next, let us look at the quintet state pathway. The first step of the reaction on the quintet PES starts with the reactants ^{5}IM0, and the second step is the formation of the hydridomethyl complex CH_3−WH (^{5}IM1) via transition state ^{5}TS01. This H transfer step is exothermic by 29.7 kcal/mol and has a barrier of 14.8 kcal/mol. Next, the ^{5}IM1 proceeds with the second H transfer to produce the quintet methylidene complex CH_2=WH_2 (^{5}IM2), which is endoergic by 26.6 kcal/mol, and has an activation barrier of 42.3 kcal/mol. The activation of the third C−H bond via the transition state ^{5}TS23 produces the methylidyne complex. This step is endoergic by 38.2 kcal/mol and has a barrier of 48.4 kcal/mol. The ^{5}IM2 can undergo reductive elimination via the planar H_2 elimination ^{5}TS24 to form the molecular complex ^{5}IM4. We located a saddle point ^{5}TS24 directly connecting the ^{5}IM2 with the ^{5}IM4. This transition structure has an imaginary frequency of 1015.18i cm^{-1}, and there is an energy barrier of 24.5 kcal/mol. The intermediate ^{5}IM4 has a W−C bond distance of 1.932 Å, as compared to the W−C bond distance in the ^{5}IM5 of 1.908 Å. The C−H bond distances are 1.093 Å for ^{5}IM4 and 1.093 Å for ^{5}IM5. The H−H bond distance is 0.772 Å compared to that of free H_2 at 0.743 Å. As for the reductive elimination step of H_2, the loosely bound H_2 molecule is easily lost. Formation of ^{5}IM5 + H_2 along this pathway is calculated to be endothermic by 1.1 kcal/mol; with no barriers in the region the hydrogen molecule is eliminated, and the tungsten−carbon system remains. To summarize, the second and the third H transfers, with barriers of 42.3 and 48.4 kcal/mol, are the rate-determining steps on the pure quintet reaction pathway. Analysis of the quintet potential energy profile shows that the first H transfer from ^{5}IM0 to CH_3−WH (^{5}IM1) appears to be an exothermic process with a reaction heat of 29.7 kcal/mol.

3.1.3. Triplet Surface of the Reaction. With respect to the triplet state pathway, the reactants (^{3}IM0) stand 31.0 kcal/mol above the septet reactants asymptote. The first H and the second H transfers are exothermic by 36.7 and 20.4 kcal/mol via the transition states ^{3}TS01 and ^{3}TS12 to generate the hydridomethyl and methylidene dihydride complexes, respectively. The C=W double bond length of 1.886 Å computed here at the B3LYP level for the tungsten methylidene dihydride complex,

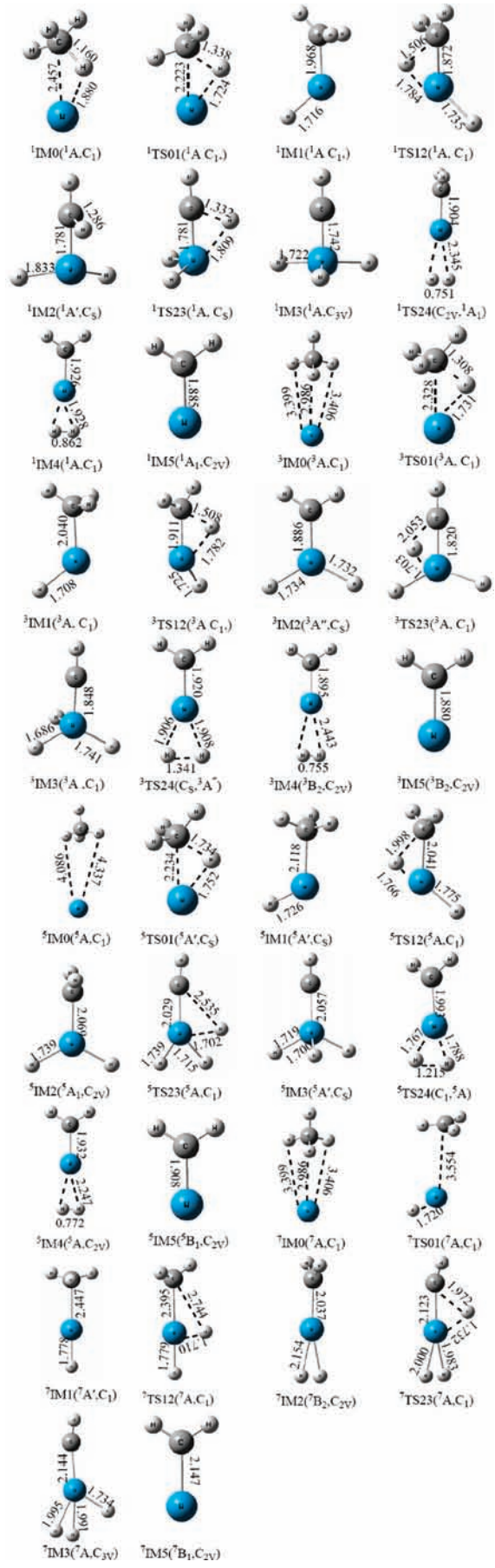

Figure 1. Structures (distances in Å) of the stationary points in the septet, quintet, triplet, and singlet states.

$CH_2{=}WH_2$. The C═W bond distance of 1.920 Å is similar to those observed for other d^0 alkylidene complexes of tungsten.[45] Finally, the third H transfer leads to the possible $CH{\equiv}WH_3$ methylidyne complex from the complex $CH_2{=}WH_2$, via the transition state ^{3}TS23. This step is endoergic by 29.7 kcal/mol and has a barrier of 35.3 kcal/mol. For the H_2 elimination path, our calculation shows that the ^{3}IM4 has to overcome a transition state (TS24) with the energy barrier of 58.0 kcal/mol and the process from ^{3}IM2 to ^{3}IM4 is endoergic by 50.1 kcal/mol. Obviously, this is not energetically and kinetically favored. The oxidative additions of the first C—H bond and the second C—H bond to form the hydridomethyl complex ^{3}IM1 and methylidene dihydride complex ^{3}IM2 are facile on the triplet pathway with barriers to reaction of 4.6 and 3.4 kcal/mol, respectively. These low barriers are noticeably different from those for the corresponding reactions that occur on the septet and quintet state pathways. The rate determining step on the triplet state PES is the third H transfer process.

3.1.4. Singlet Surface of the Reaction. Let us now move to the singlet electronic state. In the first part of the reaction a molecular adduct is formed between methane and the excited state of the W atom. As compared with ^{7}IM0, the complex ^{1}IM0 is higher in relative energy by 56.6 kcal/mol. The reaction starts from ^{1}IM0 and goes through a transition state ^{1}TS01 to reach the insertion intermediate complex ^{1}IM1 by overcoming an activation barrier of 1.3 kcal/mol (no correction of the zero-point energy). After ^{1}TS12, a downhill path can be taken on the singlet state PES, until arriving ^{1}IM3 via ^{1}TS23. The ^{1}IM1 proceeds with the second H transfer to produce the $CH_2{=}WH_2$ (^{1}IM2), which has an activation barrier of 18.0 kcal/mol. The $CH{\equiv}WH_3$ (^{1}IM3) is formed starting from the ^{1}IM2 by overcoming an activation barrier of 0.02 kcal/mol (no correction of the zero-point energy), which is considered to a barrierless mechanism. The C≡W triple bond length we have computed here at the DFT level for the new $CH{\equiv}WH_3$, 1.742 Å, which is in excellent agreement with the computed value of singlet $CH{\equiv}WH_3$ with C_{3v} symmetry,[21] compares favorably with that measured for H—C≡W in the gas phase,[46] 1.732 Å, and for the $[(t\text{-}BuO)_3W{\equiv}CMe]_2$ molecule, 1.759 Å.[47] This comparison has been made previously by Andrews and co-workers.[21] The alkylidene−tungsten separation of 1.826 Å is typical of C≡W triple bonds.[48] The overall reaction on this pathway is exothermic, 91.3 kcal/mol. The rate determining step on the singlet state PES is the third H transfer process. While the reactive is forming ^{1}IM2, if dehydrogenation is carried out, it should overcome the energy barrier of 74.4 kcal/mol, so as to form ^{1}IM4 which serves as the direct precursor for loss of H_2. As compared to breaking the third C—H bond, this step of the reaction is difficult and it would be disadvantageous to eliminate H_2.

3.2. Overview of the Stationary Points. The ground electronic state of the W atom is calculated to be a septet ^{7}S state which is associated with the s^1d^5 electronic configuration, while the quintet ^{5}D (s^2d^4) state is slightly, 5.6 kcal/mol, higher in energy at the B3LYP level of theory, which does not agree with the result of Campbell-Miller and Simard, who have reported the ^{5}D ground electronic state for the W atom.[49] This discrepancy may be due to the result of a lack of the comprehensive spin−orbit interaction in the calculations. However, our calculated value agrees well with its reported experimental value of 6.8 kcal/mol.[49] The triplet ^{3}P (s^2d^4) and singlet ^{1}S (s^2d^4) states of W are calculated to be 37.8 and 68.5 kcal/mol higher in energy than the ground state, respectively, at the B3LYP level of theory with additional RECP of Stuttgart, Table 1.

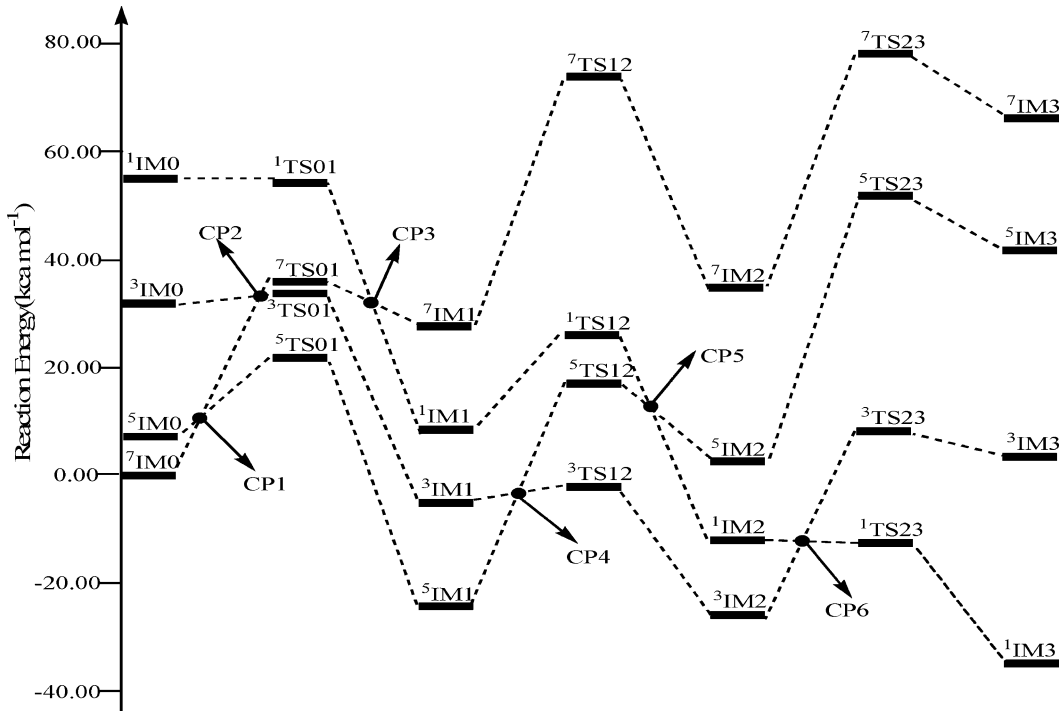

Figure 2. Potential energy surfaces of the reaction W + CH_4 → CH≡WH_3 in the septet, quintet, triplet, and singlet states.

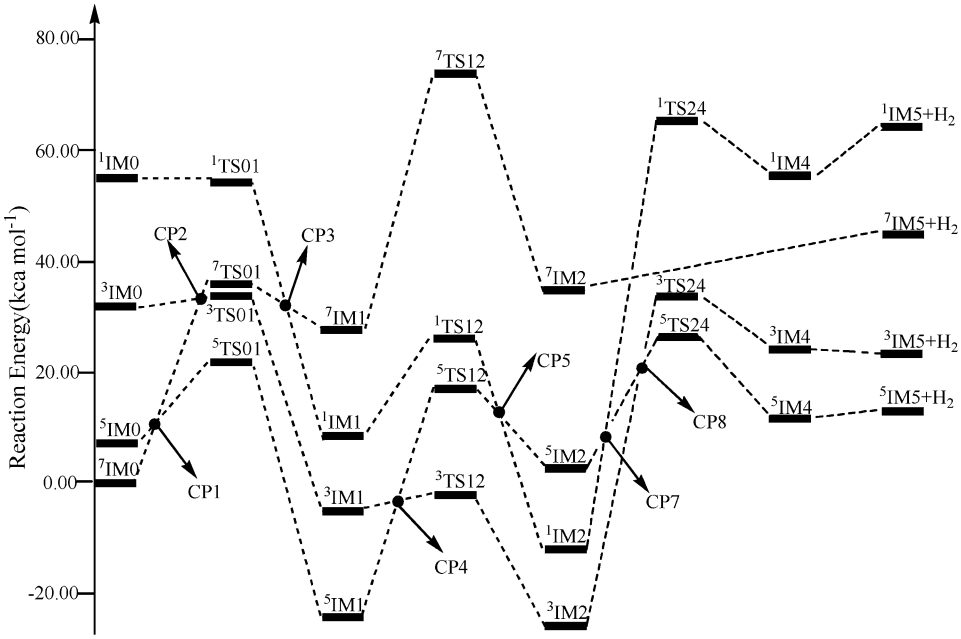

Figure 3. Potential energy surfaces of the reaction W + CH_4 → W=CH_2 + H_2 in the septet, quintet, triplet, and singlet states.

The ground state of the hydridomethyl species is a quintet state that is 52.1, 18.2, and 33.2 kcal/mol lower in relative energy than those for ^{7}IM1, ^{3}IM1, and ^{1}IM1, respectively. The C−W bond length of 2.118 Å computed here at the B3LYP level for ^{5}IM1 is the same as the computational result.[21] Natural bond orbital (NBO) calculations show that the energy differences associated with ^{7}IM1, ^{5}IM1, ^{3}IM1, and ^{1}IM1 can be mostly understood in terms of the electronic configurations associated with the metal in these four species. One sp^3 hybridization orbital of the C atom and one sd^2 hybridization orbital of the W atom are involved in the σ_{C-W} bond for ^{5}IM1. One sd^2 hybridization orbital of the W atom is involved in the σ_{H-W} bond for ^{5}IM1. The d_{xz}, d_{xy}, d_{yz}, and one sd^2 hybridization orbital of W atom are all singly occupied in ^{5}IM1, and all of them have the same spin. However, one and two of the unpaired electrons must flip over in ^{3}IM1 and ^{1}IM1 to ensure the triplet and singlet multiplicity of these species, respectively. Thus, the observed destabilization of ^{3}IM1, ^{1}IM1 relative to ^{5}IM1 is likely mainly caused by the loss of some quantum mechanical exchange effects. Since there are no vacant 5d orbitals on the W center of ^{5}IM1, the formed quintet hydridomethyl intermediate has no C−H agostic interaction. However, in the triplet and singlet hydridomethyl intermediates, the vacant 5d orbital can interact with the C−H bond of the methyl moiety. The most unstable one is the ^{7}IM1 in the species due to the evidence that no σ_{C-W} bond was found in the ^{7}IM1.

Examination of the stabilities of the spin state species of the methylene dihydride shows that ^{3}IM2 is the ground state.

TABLE 1: B3LYP/6-311++G(3df,3pd):RECP Calculated ΔE_{elec}, ΔE_{rel} for Stationary Structures Located on the Septet, Quintet, Triplet, Singlet State PESs[a]

	septet		quintet		triplet		singlet	
species	ΔE_{elec}	ΔE_{rel}	ΔE_{elec}	ΔE_{rel}	ΔE_{elec}	ΔE_{rel}	ΔE_{elec}	ΔE_{rel}
IM0	0.0	0.0	5.9	5.8	30.9	31.0	57.3	56.6
TS01	42.7	36.4	24.3	20.6	38.3	35.6	58.6	55.1
IM1	32.4	28.2	−20.3	−23.9	−1.6	−5.7	13.8	9.3
TS12	83.0	73.4	26.1	18.4	4.2	−2.3	33.8	27.3
IM2	41.4	35.4	9.5	2.7	−19.6	−26.1	−3.4	−10.8
TS23	89.0	79.0	60.8	51.1	18.5	9.2	−3.4	−11.2
IM3	76.0	67.1	50.5	40.9	12.3	3.6	−28.2	−34.7
TS24			33.6	27.2	40.3	31.9	69.8	63.6
IM4			14.8	8.5	30.8	24.0	57.6	55.2
IM5 + H_2	53.0	43.9	18.2	9.6	30.9	22.6	71.0	62.9

[a] ΔE_{elec} = relative energy (kcal mol^{-1}), ΔE_{rel} = relative energy with correction of the zero-point energy (kcal mol^{-1}).

TABLE 2: Harmonic Vibrational Frequencies Computed[a] for the Triplet Planar Ground Structure of CH_2=WH_2 and the Ground State C_{3v} Structure of CH≡WH_3

	CH_2=WH_2			CH≡WH_3	
mode description	freq[b]	int[c]	mode description	freq[b]	int[c]
CH_2 str	3151.4	0	C−H str	3235.0	14
CH_2 str	3052.3	2	W−H str	1973.1	97
WH_2 str	1920.6	169	W−H str	1961.7	245
WH_2 str	1907.7	239	W−H str	1961.6	245
CH_2 scis	1307.7	6	C≡W str	1056.2	19
WH_2 bend	891.2	24	W−H bend	847.3	23
C=W str	738.7	12	W−H bend	847.2	24
CH_2 rock	699.0	3	W≡C−H bend	737.8	25
CH_2 wag	699.4	89	W≡C−H bend	737.5	25
WH_2 wag	524.1	0	sym WH_3 def	674.9	42
WH_2 rock	246.0	67	WH_3 rock	595.9	64
CH_2 twist	97.8	0	WH_3 rock	595.7	63

[a] B3LYP/6-311++G(3df,3pd)/RECP. [b] Frequencies, cm^{-1}. [c] Intensities, km/mol.

Computed frequencies are listed in Table 2. The two strong, sharp II absorptions at 1817.2 and 1864.5 cm^{-1} are favored by near-ultraviolet irradiation.[21] The B3LYP calculation finds that the WH_2 stretching frequencies are separated by only 12.9 cm^{-1}, a value quite different from the experimental separation of 47.3 cm^{-1}, which does not fit experiment. The strongest infrared absorption of ^{5}IM1 is computed at 1908 cm^{-1}, which is the same as the lower W−H stretching mode for ^{3}IM2. Inspection of Figure 1 reveals that the C−W bond distances are 2.037 and 2.069 Å in ^{7}IM2 and ^{5}IM2, respectively. However, the C−W bond distance is 1.886 Å in ^{3}IM2. This is consistent with the calculated C−W bond length for the tungsten methylidene dilydride complex, comparing favorably with 1.874 Å computed at the CCSD level.[21] These structural parameters show that the C−W bond is quite strong in ^{3}IM2 but relatively weak in ^{7}IM2 and ^{5}IM2 which leads to the ^{7}IM2 and ^{5}IM2 higher in energy than the ^{3}IM2. The energy difference between the ^{3}IM2 and ^{1}IM2 can be attributed to their different electronic configurations determined from the NBO calculations. In both species, two p orbitals of the C atom and two 5d orbitals of W atom are involved in the $\sigma_{C=W}$ bond, while the other two 5d orbitals in ^{3}IM2 are all singly occupied; one of them has to flip over in ^{1}IM2 to ensure a singlet multiplicity for the ^{1}IM2. The vacant $5d_{x^2-y^2}$ orbital on the W center of ^{1}IM2 can attract the σ bond electrons of the C−H bond of the methylene to form a C−H agostic bond.

We next turn our attention to the methylidyne species. The C−W bond length is shorter in ^{1}IM3 (1.742 Å) than those in ^{3}IM3 (1.848 Å), ^{5}IM3 (2.057 Å), and ^{7}IM3 (2.144 Å). The relative order of the strengths of the formed C−W clearly indicated that the relative order of stability of the methylidyne complex CH≡WH_3 is ^{1}IM3 > ^{3}IM3 > ^{5}IM3 > ^{7}IM3. The calculations show that ^{1}IM3 and ^{3}IM2 are 10.8 and 2.2 kcal/mol lower in relative energy than ^{5}IM1, respectively. These results are quite consistent with the computational results by Andrews and co-workers.[21] Our B3LYP calculation shows that the strongest infrared absorption is predicted to be the doubly degenerate W−H stretching mode at 1961.7 cm^{-1} with a weaker symmetric W−H stretching mode at 1973.1 cm^{-1}. The trigonal WH_3 group exhibits two W−H stretching vibrational modes, one degenerate and one nondegenrate. The strong 1896.3 cm^{-1} and weaker 1907.5 cm^{-1} absorptions are assigned accordingly.[21] Note the agreement between the calculated 11.4 cm^{-1} and observed 11.2 cm^{-1} mode separation. Two weaker absorptions at 726.7 and 658.0 cm^{-1} exhibit the group III photochemistry, and these frequencies are appropriate for computed 737.8 and 737.5 cm^{-1} antisymmetric mostly W≡C−H bending and 674.9 cm^{-1} symmetric WH_3 deformation modes. Again, it is instructive to give a concise and qualitative description of the bonding mode in these species. The W atom uses one 6s orbital and five 5d orbitals to form three normal covalent bonds with the hydrides and one triple bond with the carbon atom in ^{1}IM3. We note that this multiconfiguration calculation gives a C_{3v} structure with a triple carbon−tungsten (σ_{CW}^2, $\pi_{CM}(1)^2$, $\pi_{CM}(2)^2$) bond. In contrast to the bonding mode in ^{1}IM3, the triple bond character of the C−W bond is reduced to some extent in ^{3}IM3, the C−W bond has double bond character in ^{5}IM3, and the C−W bond has single bond character in ^{7}IM3.

We have located three spin state species for the molecularly bound $(H_2)WCH_2$ species, namely, the quintet ^{5}IM4, the triplet ^{3}IM4, and singlet ^{1}IM4. The ^{5}IM4 is the ground state (C_{2v}) for this species. The calculated ^{3}IM4 and ^{1}IM4 are 15.5 and 46.7 kcal/mol higher in energy, respectively, than the ^{5}IM4. The NBO analysis shows that no σ_{H-W} bonds were found in this species. The $LP_{(W)} \rightarrow \sigma^*_{C-W}$ interaction between the tungsten long pair and the antiperiplanar H−H antibond is seen to give the strongest stabilization. It is found that the interaction second-order perturbation energies are 69.6, 6.9, and 14.3 kcal/mol for ^{1}IM4, ^{3}IM4, and ^{5}IM4, respectively. Thus, the hydrogen molecule elimination is the most difficult for ^{1}IM4. The ^{5}IM5 + H_2 products formed from the ground state ^{5}IM4 with no intermediate barriers are endothermic by 1.1 kcal/mol.

3.3. Crossing Points between the Multiple States. Figures 2 and 3 depict the computed potential energy diagrams for the activation of methane in the septet, quintet, triplet, and singlet states. Examination of Figures 2 and 3 shows that the different C−H bond activation processes display completely different

preferences for the reaction barriers on the four energy surfaces. In the preceding discussion, we can see that the minimum energy overall PES is not one of the four PESs of a certain spin state. Thus, the crossing of surfaces of different spins is likely involved in the overall C−H bond activation by the W atom. We note that transition metal mediated reactions very often occur on more than one PES. This has attracted some experimental and theoretical attempts in reaction systems that include 3d, 4d, and some 5d transition metals.

As seen in Figures 2 and 3, eight crossing points may be found to be possible along the optimal reaction pathway of the activation of CH_4, for the $^7W + CH_4 \rightarrow {}^1CH{\equiv}WH_3$ and H_2 elimination path, because the SOC matrix element is zero if the spins for the bra and ket differ by more than unity ($|S - S'| > 1$).[50] Therefore, the probability of surface hopping at CP2, CP3, CP5, and CP7 is ineffective, the reactions seem to take place with no change in the spin angular momentum, and the spin-forbidden channels are not relevant. The other four crossing points obtained between the septet and quintet states (CP1), between the quintet and triplet states (CP4), between the triplet and singlet states (CP6), and between the triplet and quintet state (CP8) may play a key role on the nonadiabatic processes.

The existence of MECP1 (CP1) opens the possibility for an ISC to take place. When the reaction reaches the vicinity of MECP1, the state of MECP1 in the high spin state may mix with that in the low spin state, which will decrease the activation barrier. The values of the spin densities of MECP1 are different on both PESs. In the septet state, MECP1 presents large values at the tungsten center (5.94 au) and the CH_4 atom center (0.06 au). In the quintet state, their spin densities are 3.93 and 0.07 au, respectively. Therefore, a change of the spin pairing on the W and CH_4 is necessary in the septet state to reach the quintet state. From this point onward, the reaction can be continued on the quintet state PES as a low-cost reaction pathway toward the hydridomethyl complex ^{5}IM1. It must be noted that MECP1 is reached before the rate-limiting step of the resulting pathway, and therefore the spin inversion can be kinetically relevant, because it takes place in the entrance channel.

It can be seen from Figure 2 that the relative potential energy of ^{5}IM1/^{3}IM2 is more stable by 18.2/15.3 kcal/mol than ^{3}IM1/^{1}IM2, but the transition state ^{5}TS12/^{3}TS23 stands 20.7/20.4 kcal/mol above the transition state ^{3}TS12/^{1}TS23, so there is an energy crossing phenomenon before the transition state. Namely, the probability of spin inversion is moderate to allow for an efficient conversion to the most favorable energetic surface along the reaction path. The ISC, via MECP4 (CP4), between the quintet and triplet PESs occurs during the path connecting ^{3}TS12 with the stable intermediate ^{5}IM1. The molecular system may change its spin multiplicity from the quintet to the triplet state at this point. That is, after MECP4, the triplet PES can provide a low-cost reaction pathway toward the methylidene complex ^{3}IM2. At the same time, the existence of MECP6 (CP6) also strongly verifies that the reaction path transfers to the singlet PES and the eventual product ^{1}IM3 is formed.

As can be seen in Figure 3, the products in quintet state, ^{5}IM5 + H_2, will be formed from the ground ^{3}IM2 in the triplet. Therefore, at least a crossing and spin inversion process should take place in the reaction pathway. The ISC, via MECP8 (CP8), between the triplet and quintet PESs occurs during the path connecting ^{5}TS24 with the stable intermediate ^{3}IM2. From the MECP8, the reaction could be continued on the quintet state PES and the ^{5}IM4 may be found as a stable minimum $(H_2)WCH_2$. Finally, the hydrogen molecule is eliminated, and the tungsten−carbon system remains $W{=}CH_2$ (^{5}IM5).

Putting all the findings together, the overall potential energy profiles for the spin-forbidden reaction $^7W + CH_4 \rightarrow {}^1CH{\equiv}WH_3$ or $^7W + CH_4 \rightarrow {}^5W{=}CH_2 + H_2$ may be possible along the optimal reaction pathway. First, the reaction may start with the formation of the hydridomethyl complex ^{5}IM1 through ISC at MECP1 between the septet and the quintet state. Then, the quintet surface could likely cross the triplet surface at MECP4 between ^{5}IM1 and ^{3}TS12 since ^{5}TS12 is too high in energy and the formation of the complex ^{3}IM2 is exothermic on the triplet PES instead of endothermic on the quintet PES. After ^{3}IM2 is formed, the reaction may follow by ISC at MECP6 from the triplet to the singlet PES to reach the last transition state ^{1}TS23 or by ISC at MECP8 from the triplet to the quintet PES to reach the last transition state ^{5}TS24, since ^{3}TS23 is 20.4 kcal/mol above ^{1}TS23 or ^{5}TS24 is 4.7 kcal/mol below ^{3}TS24. On the other hand, the complex ^{1}IM3 on the singlet PES is thermodynamically more favored than the corresponding triplet state species. In the hydrogen molecule eliminated region, the $W{=}CH_2$ (^{5}IM5) + H_2 products are endothermic by 6.9 kcal/mol but by 48.7 kcal/mol for the hydrogenation products, $W{=}CH_2$ (^{3}IM5) + H_2. To conclude, the minimum energy pathway may proceed as $W(^7S) + CH_4 \rightarrow$ MECP1 $\rightarrow {}^5$TS01 $\rightarrow CH_3{-}WH$ (^{5}IM1) $\rightarrow$ MECP4 $\rightarrow {}^3$TS12 $\rightarrow CH_2{=}WH_2$ (^{3}IM2) $\rightarrow$ MECP6 $\rightarrow {}^1$TS23$\rightarrow CH{\equiv}WH_3$ (^{1}IM3) and $W(^7S) + CH_4 \rightarrow$ MECP1 $\rightarrow {}^5$TS01 $\rightarrow CH_3{-}WH$ (^{5}IM1) $\rightarrow$ MECP4 $\rightarrow {}^3$TS12 $\rightarrow CH_2{=}WH_2$ (^{3}IM2) $\rightarrow$ MECP8 $\rightarrow {}^5$TS24$\rightarrow W{=}CH_2$ (^{5}IM5) + H_2.

Our calculated reaction pathway is consistent with Andrews' experimental results. The visible irradiation (>530 nm, ∼54 kcal/mol) drives the W + CH_4 reaction straightforward to the lowest-energy $CH{\equiv}WH_3$ molecule.[21] However, the UV irradiation (240−380 nm, ∼100 kcal/mol) restores $CH_3{-}WH$ and $CH_2{=}WH_2$ molecules at the expense of $CH{\equiv}WH_3$.[21] As we estimated, the minimum energy barriers for insertion reactions are 20.6, 21.6, and 14.8 kcal/mol, respectively. Apparently the 530 nm irradiation is too high to provide evidence for our calculated minimum reaction pathway. On the basis of our calculation we estimated near-infrared irradiation can initiate the reactions if the absorptions of the precursors are available in this range. The calculated ^{5}IM3 and ^{5}TS23 species are located 75.6 and 85.8 kcal/mol higher than ^{1}IM3 ($CH{\equiv}WH_3$) that can be excited through near-ultraviolet irradiation to pass ^{5}TS23 to give ^{5}IM2, and then relax to ^{3}IM2 ($CH_2{=}WH_2$), which matches the experimentally observed restoration process very well. The same near-ultraviolet can also excite ^{3}IM2 ($CH_2{=}WH_2$) to ^{7}IM2, which passes the ^{7}TS12 transition state to give ^{7}IM1 and then relax to ^{5}IM1 ($CH_3{-}WH$).

3.4. Mechanistic Aspects in MECP. Many theoretical investigations[51,52] have manifested the principal mechanism which mixes the two spin states and provides probability of ISC is SOC. The first crossing seam that exists prior to TS01 is the important aspect in this reaction pathway because the molecular system should change its spin multiplicity from the septet to the quintet state near this crossing region, leading to a significant decrease in the barrier height of TS01 from 36.4 to 20.6 kcal/mol. Ideally, large SOC occurs when the electronic transition that accompanies the spin flip creates orbital angular momentum. For MECP1, the computed SOC constant is 572.5 cm^{-1}, obtained by using a one-electron spin−orbit Hamiltonian in GAMESS.[41] As a consequence, the ISC at MECP1 occurs efficiently because of the strong SOC involved. In most of these nonadiabatic processes, the nonadiabatic transition probability is given by the well-known Landau−Zener (LZ) formula for the two-state curve crossing problem. However, it is well-known

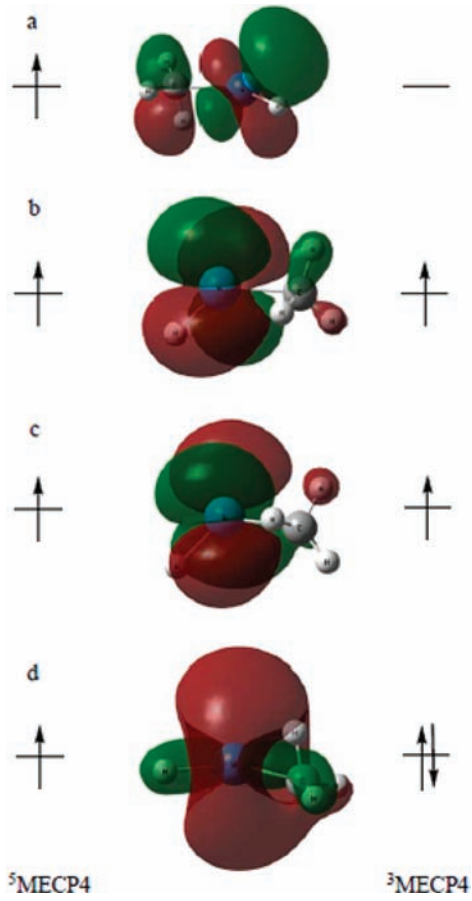

Figure 4. Frontier molecular orbital interaction analyses for MECP4.

that the LZ theory does not work at energies near or lower than the crossing point; it does not incorporate the effects of nonadiabatic tunneling. Thus, we have not estimated the probability of hopping from the septet state surface to the quintet state surface in the vicinity of the crossing region.

The spin inversion from the quintet to the triplet state can occur in the vicinity of the forth crossing seam of two PESs of different spin multiplicities. The barrier of activation of the third H-transfer requires 42.3 kcal/mol if the reaction proceeds only on the quintet PES. However, if the spin multiplicity of the molecular system is changed from the quintet to the triplet state, the activation energy barrier can be significantly decreased to 21.6 kcal/mol. In order to have a deep understanding of the crossing and the spin inversion, we have gained useful information about MECP4 from the frontier molecular orbital interaction analyses. When the reaction reaches the vicinity of MECP4, the state of ^{5}MECP4 may mix with that of ^{3}MECP4, which will decrease the activation barrier, leading to a rate acceleration.

In Figure 4, the a orbital is the d_{xz} orbital of W, which is the highest single occupied orbital (HOMO) in quintet state, but is the lowest empty orbital (LUMO) in triplet state. The b orbital is the lowest singly occupied orbital (SOMO) composed of W d_{z^2} in the quintet state, which is the highest double occupied orbital in the triplet state. In the present case, the α electron in the d_{xz} orbital will undergo spin inversion. In other words, the single electron leaps from the W $5d_{xz}$ orbital to the W $5d_{z^2}$ orbital. Because this single electron in an atom transfer at a different orbital is allowed,[53] the ISC is efficient. In the present work, an estimate of the probability of ISC from one state to the other state can be obtained using a semiclassical picture based on potential energy surfaces, where the probability of surface hopping through the crossing point is given by the Landau−Zener-type model given in the Computational Details section. For the calculation of $\vec{v}$, it is assumed that the excess excitation energy is converted into kinetic energy, and the corresponding velocity vector is parallel to the gradient difference vector. For MECP, the computed SOC is 2369.6 cm^{-1}. Using this approximation, the calculated values for $\vec{g}d$ and $\vec{v}$ are 0.030015 hartree bohr^{-1} and 0.006579 bohr per atomic time unit, respectively. On the basis of the calculated SOC value and potential energy surfaces, the probability of ISC (P^{ISC}) for a single passage through the ISC region is approximately 0.975. The spin inversion from the quintet to the triplet state takes place easily at MECP4 due to the large values of P^{ISC} estimated.

There is a crossing seam that exists between the triplet and singlet states in the exit channel, in which the complex ^{1}IM3 containing a triple carbon−metal bond is formed via a H-transfer process. A spin inversion from the triplet to the singlet state will again occur in the vicinity of the crossing seam. An important consequence of this spin inversion is that the barrier height of TS23 decreases from 35.3 to 14.8 kcal/mol. According to the above method, the computed SOC is 1340.2 cm^{-1}.The large probabilities ($P^{ISC} = 0.916$) at MECP6 were also calculated with the $\vec{g}d$ and $\vec{v}$ as 0.032789 hartree bohr^{-1} and 0.002878 bohr per atomic time unit, respectively.

Armed with the potential-energy surfaces of Figure 3, the mechanism for the dehydrogenation of methane in the presence of one W atom is clear. Formation of ground state W═CH_2 (^{5}IM5) + H_2 products must correspond to ^{3}IM2. Therefore, there must be a crossing from the triplet to the quintet state. MECP8 exists between the ^{3}IM2 and the ^{5}TS24. The SOC matrix element was found to be, irrespective of its sign, 887.0 cm^{-1}. If ISC at MECP8 occurs, the activation energy barrier can be slightly decreased from 58.0 to 53.3 kcal/mol. As the hydrogenation products, W═CH_2 (^{5}IM5) + H_2, are 9.6 kcal/mol above the ground reactant asymptote, methane dehydrogenation in the presence of one W atom is endothermic. Obviously, this is not energetically and kinetically favored. The calculations make a clear prediction that the product of the reaction is ^{3}IM2 rather than H_2 elimination. Because the hydrogen molecule elimination is difficult, it is not necessary to discuss the probability of ISC at MECP8. A new lower energy pathway was identified for the CH_4 dehydrogenation on a Pt atom, which is endothermic by 10.4 kcal/mol.[54] A small energy barrier, 7.4 kcal/mol, has to be overcome to form the H_2−Pt−CH_2 complex through the transition state, which is 2.8 kcal/mol above the reactant asymptote.[54] As compared to the CH_4−Pt system, this illustrated that W is less active toward CH_4 dissociation due to a large potential barrier.

As mentioned above, from the point of view of energy and the surface hopping probability, the reaction $^7W + CH_4 \rightarrow {}^1CH{\equiv}WH_3$ passes through three effective MECPs, the reaction $^7W + CH_4 \rightarrow {}^5W{=}CH_2 + H_2$ also passes through three MECPs, and the minimum reaction pathway is apparently favorable case for ISC. As the crossing takes place before the transition states, the effective spin inversion will make the reaction accessible to a lower energy pathway, leading to a rate acceleration. Therefore, the spin inversion acts as a mechanistic distributor, and it is responsible for the reaction efficiency.

4. Conclusion

CH_4 activation by W in the Gas phase is a typical "two-state reactivity" (TSR) reaction. The crossing points between the PESs and possible spin inversion processes for the direct conversion of methane to a high oxidation state transition metal complex

that contains a carbon−metal double or triple bond are investigated. There are three main effective MECPs along the overall reaction pathway, and the reaction system would likely change its spin multiplicity three times in going from the entrance channel to the exit channel. The first MECP is the important aspect in this reaction pathway because the molecular system should change its spin multiplicity from the septet to the quintet state near this crossing region, leading to a significant decrease in the barrier height of TS01 from 36.4 to 20.6 kcal/mol. The fourth MECP occurs in the process of the second H-transfer, which can result in a large decrease in the barrier height of TS12 from 42.3 to 21.6 kcal/mol. The sixth crossing seam exists in the exit channel and will again lead to spin inversion from the triplet to the singlet state, by which the barrier of activation of the third H-transfer can be decreased from 35.3 to 14.8 kcal/mol. Thus, the ISC has become energetically allowable. The minimum energy reaction path is found not to be one of the four PESs of a certain spin state. The minimum energy pathway can be described as $W(^7S) + CH_4 \rightarrow$ MECP1 $\rightarrow$ ^{5}TS01 $\rightarrow$ CH_3—WH (^{5}IM1) $\rightarrow$ MECP4 $\rightarrow$ ^{3}TS12 $\rightarrow$ CH_2═WH_2 (^{3}IM2) $\rightarrow$ MECP6 $\rightarrow$ ^{1}TS23 $\rightarrow$ CH≡WH_3 (^{1}IM3). The calculated energy pathway is exothermic which is in good agreement with the experimental and the computational results from Andrews' group.[21]

The calculations explore the septet, quintet, triplet, and singlet PESs along paths leading from W + CH_4 to the breaking C—H bond and onward to elimination of H_2. The minimum energy pathway can be described as $W(^7S) + CH_4 \rightarrow$ MECP1 $\rightarrow$ ^{5}TS01 $\rightarrow$ CH_3—WH (^{5}IM1) $\rightarrow$ MECP4 $\rightarrow$ ^{3}TS12 $\rightarrow$ CH_2═WH_2 (^{3}IM2) $\rightarrow$ MECP8 $\rightarrow$ ^{5}TS24 $\rightarrow$ W═CH_2 (^{5}IM5) + H_2. The value of calculated heat of the methane dehydrogenation in the presence of one W atom is 9.6 kcal/mol with the highest TS activate energy of 53.3 kcal/mol. This fact suggests that the title reaction is unfavorable from kinetic and thermodynamic viewpoints. The calculations make a clear prediction that the product of the reaction is ^{3}IM2 rather than H_2 elimination.

Moreover, we have calculated the surface hopping probability at MECP4 and MECP6; this provides valuable support for the spin-forbidden reaction as it can be established that the reaction of W and CH_4 should proceed on the multistate surface with spin change. For the MECPs, the computed SOC matrix elements are very strong in these regions. The large values of P^{ISC} passes estimated show that the ISC occurs with a greatly probability. As a consequence, ISC takes place with a large probability.

Acknowledgment. This work is supported by the National Natural Science Foundation of China (Grant 20873102).

Supporting Information Available: Geometries of the stationary points at the septet, quintet, triplet, and singlet states. This material is available free of charge via the Internet at http://pubs.acs.org.

References and Notes

(1) Rostrup-Nielsen, J. R. *Catal. Today* **2000**, *63*, 159.
(2) Lunsford, J. H. *Catal. Today* **2000**, *63*, 165.
(3) Choudharly, T. V.; Aksoylu, E.; Goodman, D. W. *Catal. Rev.* **2003**, *45*, 151.
(4) Janowicz, A. H.; Bergman, R. G. *J. Am. Chem. Soc.* **1982**, *104*, 352.
(5) Shilov, A. E.; Shul'pin, G. B. *Chem. Rev.* **1997**, *97*, 2879.
(6) Davies, H. M. L.; Beckwith, R. E. J. *Chem. Rev.* **2003**, *103*, 2861.
(7) Irikura, K. K.; Beauchamp, J. L. *J. Am. Chem. Soc.* **1991**, *113*, 2769.
(8) Crabtree, R. H. *Chem. Rev.* **1985**, *85*, 245.
(9) Crabtree, R. H. *Chem. Rev.* **1995**, *95*, 987.
(10) Schrock, R. R. *Chem. Rev.* **2002**, *102*, 145.
(11) Buchmeiser, M. R. *Chem. Rev.* **2000**, *100*, 1565.
(12) Tran, E.; Legzdins, P. *J. Am. Chem. Soc.* **1997**, *119*, 5071.
(13) Irikura, K. K.; Beauchamp, J. L. *J. Am. Chem. Soc.* **1989**, *111*, 75.
(14) Ranasinghe, Y. A.; MacMahon, T. J.; Freiser, B. S. *J. Phys. Chem.* **1991**, *95*, 7721.
(15) Andrews, L.; Cho, H.-G.; Wang, X. *Inorg. Chem.* **2005**, *44*, 4834.
(16) Cho, H.-G.; Wang, X.; Andrews, L. *Organometallics* **2005**, *24*, 2854.
(17) Andrews, L.; Cho, H.-G.; Wang, X. *Angew. Chem., Int. Ed.* **2005**, *44*, 113.
(18) Cho, H. G.; Wang, X.; Andrews, L. *J. Am. Chem. Soc.* **2005**, *127*, 465.
(19) Cho, H.-G.; Andrews, L. *J. Phys. Chem. A* **2006**, *110*, 3886.
(20) Cho, H.-G.; Andrews, L. *J. Am. Chem. Soc.* **2005**, *127*, 8226.
(21) Cho, H.-G.; Andrews, L.; Marsden, C. *Inorg. Chem.* **2005**, *44*, 7634.
(22) Carroll, J. J.; Haug, K. L.; Weisshaar, J. C. *J. Phys. Chem.* **1995**, *99*, 13955.
(23) Svensson, M.; Blomberg, M. R. A.; Siegbahn, P. E. M. *J. Am. Chem. Soc.* **1991**, *113*, 7076.
(24) Blomberg, M. R. A.; Siegbahn, P. E. M.; Svensson, M. *J. Am. Chem. Soc.* **1992**, *114*, 6095.
(25) Carroll, J. J.; Haug, K. L.; Weisshaar, J. C. *J. Am. Chem. Soc.* **1993**, *115*, 6962.
(26) Carroll, J. J.; Weisshaar, J. C. *J. Phys. Chem.* **1996**, *100*, 12355.
(27) de Alemeida, K. J. ; Cesar, A., *Organometallics* **2006**, *25*, 3407.
(28) Yang, H. Q.; Chen, Y. Q.; Hu, C. W.; Gong, M. C.; Hu, H. R.; Tian, A. M.; Wong, N. B. *Chem. Phys. Lett.* **2002**, *355*, 233.
(29) Campell, M. L. *Chem. Phys. Lett.* **2002**, *365*, 361.
(30) Schröder, D.; Shaik, S.; Schwarz, H. *Acc. Chem. Res.* **2000**, *33*, 139.
(31) Poli, R.; Harvey, J. N. *Chem. Soc. Rev.* **2003**, *32*, 1.
(32) Armentrout, P. B. *Science* **1991**, *251*, 175.
(33) Yarkony, D. R. *J. Phys. Chem.* **1996**, *100*, 18612.
(34) Frisch, M. J.; Trucks, G. W.; Schlegel, H. B.; et al. *Gaussian 03, revision-E.01*; Gaussian Inc.: Pittsburgh, PA, 2003.
(35) Becke, A. D. *J. Chem. Phys.* **1993**, *98*, 5648.
(36) Becke, A. D. *Phys. Rev. A* **1988**, *38*, 3098.
(37) Lee, C.; Yang, W.; Parr, R. G. *Phys. Rev. B.* **1988**, *37*, 785.
(38) McLean, A. D.; Chandler, G. S. *J. Chem. Phys.* **1980**, *72*, 5639.
(39) Yoshizawa, K.; Shiota, Y.; Yamabe, T. *J. Chem. Phys.* **1999**, *111*, 538.
(40) Harvey, J. N.; Aschi, M.; Schwarz, H.; Koch, W. *Theor. Chem. Acc.* **1998**, *99*, 95.
(41) Schmidt, M. W.; Baldridge, K. K.; Boatz, J. A.; Elbert, S. T.; Gordon, M. S.; Jensen, J. H.; Koseki, S.; Matsunaga, N.; Matsunaga, K. A.; Nguyen, K. A.; Su, S. J.; Windus, T. L.; Dupulis, M.; Montgomery, J. A. *J. Comput. Chem.* **1993**, *14*, 1347.
(42) Koseki, S.; Gordon, M. S.; Schmidt, M. W.; Matsunaga, N. J. *J. Phys. Chem.* **1995**, *99*, 12764.
(43) Manaa, M. R.; Yarkony, D. R. *J. Chem. Phys.* **1991**, *95*, 1808.
(44) Manuela, M.; Luis, S. A.; Michael, A, R.; Llus, B *J. Am. Chem. Soc.* **2005**, *127*, 1820.
(45) Chem, T. N.; Wu, Z. Z.; Sorasaenee, K. R.; Diminnie, J. B.; Pan, H. J; et al. *J. Am. Chem. Soc.* **1998**, *120*, 13519.
(46) Barnes, M.; Gillett, D. A.; Merer, A. J.; Metha, G. F. *J. Chem. Phys.* **1996**, *105*, 6168.
(47) Chisholm, M. H.; Hoffman, D. M.; Huffman, J. C. *Inorg. Chem.* **1983**, *22*, 2903.
(48) Anderson, S.; Cook, D. J.; Hill, A. F.; Malget, J. M.; White, A. J. P.; Williams, D. J. *Organometallics.* **2004**, *23*, 2552.
(49) Campbell-Miller, M. D.; Simard, B. *J. Opt. Soc. Am. B.* **1996**, *13*, 2115.
(50) Fedorov, D. G.; Koseki, S.; Schmidt, M. W.; Gordon, M. S. *Int. Rev. Phys. Chem.* **2003**, *22*, 551.
(51) Ermler, W. C.; Ross, R. B.; Christiansen, P. A. *Adv. Quantum Chem.* **1988**, *19*, 139.
(52) Danovich, D.; Shaik, S. *J. Am. Chem. Soc.* **1997**, *119*, 1773.
(53) Turro, N. J. *Modern Molecular Photochemistry*, Science Press, Beijing, 1987.
(54) Xiao, L.; Wang, L. C. *J. Phys. Chem. B.* **2007**, *111*, 1657.

JP9054439